The EMBO Journal Vol.17 No.22 pp.6437–6448, 1998

Structural origins of gentamicin antibiotic action

Satoko Yoshizawa, Dominique Fourmy[1] and Joseph D.Puglisi[2]

Department of Structural Biology, Stanford University School of Medicine, Stanford, CA 94305-5400, USA

[1]Present address: Laboratoire de RMN, CNRS ICSN, 1 Avenue de la terrasse, 91190 Gif-sur-Yvette, France

[2]Corresponding author
e-mail: puglisi@stanford.edu

Aminoglycoside antibiotics that bind to the ribosomal A site cause misreading of the genetic code and inhibit translocation. The clinically important aminoglycoside, gentamicin C, is a mixture of three components. Binding of each gentamicin component to the ribosome and to a model RNA oligonucleotide was studied biochemically and the structure of the RNA complexed to gentamicin C1a was solved using magnetic resonance nuclear spectroscopy. Gentamicin C1a binds in the major groove of the RNA. Rings I and II of gentamicin direct specific RNA–drug interactions. Ring III of gentamicin, which distinguishes this subclass of aminoglycosides, also directs specific RNA interactions with conserved base pairs. The structure leads to a general model for specific ribosome recognition by aminoglycoside antibiotics and a possible mechanism for translational inhibition and miscoding. This study provides a structural rationale for chemical synthesis of novel aminoglycosides.

Keywords: aminoglycoside antibiotics/gentamicin/NMR spectroscopy/ribosome/16S rRNA

Introduction

The ribosome is the target of many clinically important antibiotics. These compounds, which include aminoglycosides, tetracyclines and macrolides, interfere with essential steps of protein synthesis. The RNA components of ribosomes are central to their catalytic function, and functional sites are highly conserved among organisms (Noller, 1991). Most antibiotics that bind to the ribosome have been shown to interact with ribosomal RNA (Moazed and Noller, 1987a,b; Woodcock *et al*., 1991). The complex three-dimensional folds of RNA represent specific targets for small molecule drug recognition, yet the high conservation of functional sites across species suggests problems of toxicity.

Aminoglycosides are the best characterized class of antibiotics that bind directly to ribosomal RNA (Figure 1). Aminoglycosides cause decreases in translational accuracy and inhibit translocation of the ribosome (Davies *et al*., 1965; Davies and Davis, 1968). Aminoglycoside antibiotics bind to a conserved sequence of rRNA that is near the site of codon–anticodon recognition in the aminoacyl-tRNA site (A site) of 30S subunits (Figure 2). Aminoglycoside binding stabilizes the tRNA–mRNA interaction in the A site by decreasing tRNA dissociation rates, which interferes with proofreading steps that ensure translational fidelity (Karimi and Ehrenberg, 1994). Besides their medical importance, aminoglycoside antibiotics have provided insights into ribosome function.

Though chemically distinct, related aminoglycoside antibiotics all bind in the ribosomal A site (Figure 1). Aminoglycosides are positively charged at biological pH (Botto and Coxon, 1983), which contributes to RNA binding. A comparison of the antibiotics suggests chemical groups that are essential for aminoglycoside function (Benveniste and Davies, 1973). Rings I and II are the most common moieties of the aminoglycosides, although their substitution patterns may differ. The N1 and N3 amino groups of ring II (2-deoxystreptamine) are common to all aminoglycosides, as are hydrogen-bond donors at the 2′ and 6′ positions of ring I. The linkage of ring III to 2-deoxystreptamine can vary. In the neomycin class, including aminoglycosides such as ribostamycin and paromomycin, ring III is connected to position 5 of ring II (4,5-disubstituted ring II), whereas in the kanamycin class, including the gentamicins, ring III is linked to position 6 of ring II (4,6-disubstituted ring II). Rings III of the kanamycin class aminoglycosides share common chemical groups at the 2′′ and 3′′ positions. Among aminoglycosides, the total number of rings can also vary from two to four. A large group of enzymes covalently modifies aminoglycosides to yield resistance (Shaw *et al*., 1993). These modifications, which include acetylation of amino groups and phosphorylation and adenylation of hydroxyl groups, occur primarily on rings I and II.

The interaction between the aminoglycoside antibiotic paromomycin and the A site was previously characterized biochemically using an RNA molecule (27 nucleotides) containing the target site for these antibiotics (Recht *et al*., 1996) (Figure 2). The solution structure of this RNA molecule alone and that of the complex with paromomycin were solved by nuclear magnetic resonance (NMR) (Fourmy *et al*., 1996, 1998b). The antibiotic binds in the major groove of the RNA within a pocket created by an A1408·A1493 base pair and a single bulged adenine (A1492). Specific interactions occur between chemical groups of rings I and II of paromomycin and the conserved nucleotides in the RNA. The related aminoglycosides, neomycin, ribostamycin and neamine, that have a common core of rings I and II, bind in a qualitatively similar manner to the A-site RNA as paromomycin (Fourmy *et al*., 1998a). These studies explained the molecular basis for the interaction of 4,5-disubstituted ring II (neomycin class) aminoglycosides and 16S rRNA.

All clinically useful aminoglycosides contain a

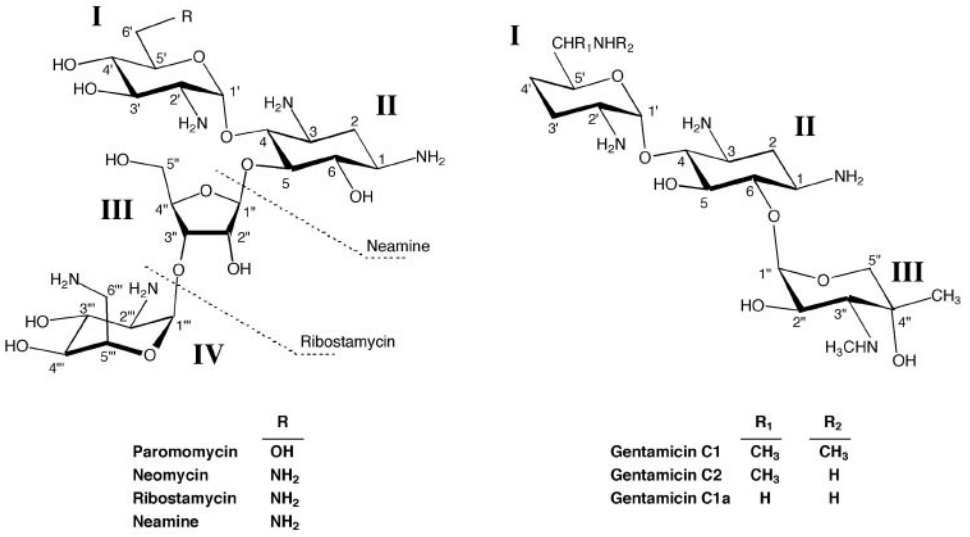

Fig. 1. Structures of the aminoglycoside antibiotics that bind in the A site of 16S rRNA. Comparison of the gentamicin components (4–6 ring II–ring I, ring II–ring III linkages) and the neomycin group (4–5 ring II–ring I, ring II–ring III linkages) of aminoglycosides. The neomycin group includes paromomycin, neomycin, ribostamycin and neamine. Ribostamycin contains all rings except ring IV while neamine lacks both rings III and IV.

4,6-disubstituted ring II (kanamycin class). Gentamicin C is a representative of this class of aminoglycosides and is a mixture of three components, gentamicin C1a, C2 and C1, that have different patterns of methylation at the 6′ position of ring I (Figure 1). In addition, ring I of the gentamicin C components lacks the 3′ and 4′ hydroxyl groups compared with ring I of paromomycin. These 3′, 4′ and 6′ hydroxyl groups are involved in the interaction with A-site RNA in the paromomycin–A-site RNA structure. The different chemical structures of gentamicin C allow us to test the roles of ring I substituents and different ring II–ring III linkages on aminoglycoside–RNA affinity.

To understand better how aminoglycoside antibiotics bind to ribosomal RNA and interfere with translation, and to understand the superiority of the 4,6-disubstituted class as drugs, we have characterized the interaction of gentamicin C components with the ribosome and with the model A-site RNA oligonucleotide using biochemical and biophysical methods. Furthermore, we present the NMR structure of a gentamicin C1a–A-site oligonucleotide complex.

Results

Binding of gentamicin components to the 30S ribosomal subunit

The three components of gentamicin C were purified from the mixture and the binding of each component of gentamicin C to 30S subunits was assayed by chemical probing with dimethyl sulfate (DMS) at pH 7.2. Each component of gentamicin C protects the same bases of 16S rRNA from modification, although the protections are observed at different concentrations (Figure 3A). A weak footprint is observed at G1494(N7) and A1408(N1) in the presence of 1 μM gentamicin C1a and 10 μM gentamicin C2. The intensity of the gentamicin C1 footprint is weaker and the concentration of antibiotic required to observe the footprint is higher (100 μM). The same bases of 16S rRNA were previously shown to be protected by binding of the gentamicin C mixture to 30S subunits

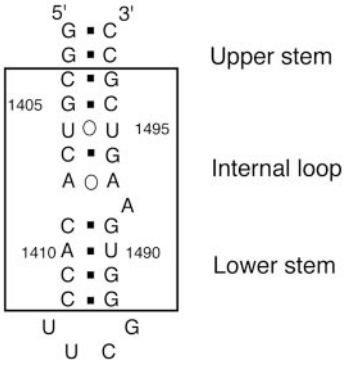

Fig. 2. The secondary structure of an oligonucleotide that corresponds to *E.coli* 16S rRNA in the region of the A site. The natural sequence is boxed.

(Moazed and Noller, 1987a). The difference in the affinity of gentamicin C1a and C1 explains their relative inhibitory effects on translation *in vitro (*Benveniste and Davies, 1973).

The three components of gentamicin C bind to the 30S ribosomal subunit at the same binding site but with different affinities; gentamicin C1a binds to 30S subunits with slightly higher affinity than C2, whereas C1 binds with the lowest affinity compared the others. A 27 nucleotide A-site oligomer (Figure 2) was shown previously to mimic aminoglycoside antibiotic interaction with the ribosome and to be a convenient tool to measure the K_ds of aminoglycoside–rRNA complexes (Recht *et al*., 1996; Fourmy *et al*., 1998a). The same oligonucleotide was used here to study the gentamicin interaction with the A site.

Binding of gentamicin components to an A-site model oligonucleotide

The interaction of each gentamicin component with the A-site oligonucleotide was assayed by chemical probing with DMS at pH 7.0. It was shown previously that in the presence of 10 μM paromomycin, residues G1405, A1408 and G1494 were strongly protected from chemical modi-

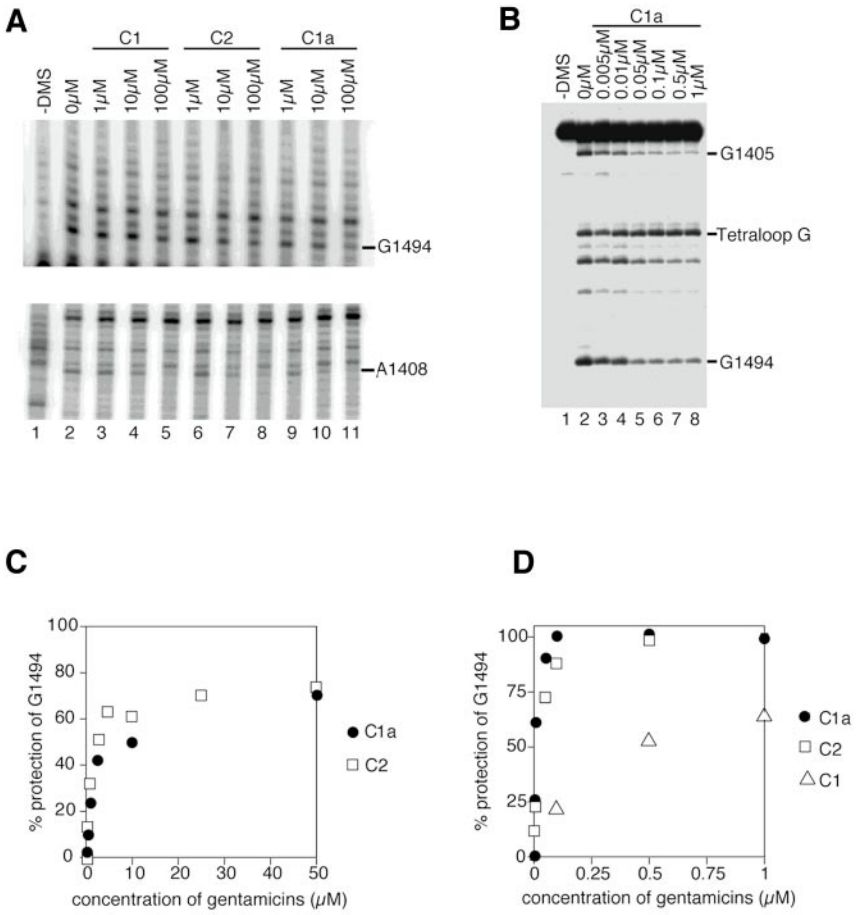

Fig. 3. (**A**) Autoradiograph of DMS probing reactions on 30S ribosomal subunits. Lane 1 is a control reaction with no DMS added. Lane 2 is a DMS probing reaction in the absence of gentamicin. Subunits were present at a concentration of 100 nM in all reactions. Lanes 3–5 are reactions in the presence of 1, 10 and 100 μM gentamicin C1, respectively. Lanes 6–8 are reactions in the presence of 1, 10 and 100 μM gentamicin C2, respectively. Lanes 9–11 are reactions in the presence of 1, 10 and 100 μM gentamicin C1a, respectively. Bands corresponding to nucleotides G1494 and A1408 are indicated. (**B**) Autoradiograph of DMS probing reactions on 3′ end-labeled 27 nt RNA. In all reactions, the oligonucleotide is present at a concentration of 5 nM. DMS probing reactions were carried out on ice. Lane 1 is a control reaction with no DMS added. Lane 2 is a DMS probing reaction in the absence of gentamicin. Lanes 3–8 are reactions in the presence of 0.005, 0.01, 0.05, 0.1, 0.5 and 1 μM gentamicin C1a, respectively. (**C**) Graph showing the reactivity to DMS at G1494(N7) at 25°C as a function of increasing gentamicin C1a (●) and C2 (□) concentration. Reactivity between lanes was normalized using the reactivity of the tetraloop G as the standard. (**D**) Graph showing the reactivity to DMS at G1494(N7) at 0°C as a function of increasing gentamicin C1a (●), C2 (□) and C1 (△) concentration. Reactivity between lanes was normalized using the reactivity of the tetraloop G as the standard.

fication by DMS whereas G1491 and G1497 were weakly protected, with an estimated K_d of 0.2 μM (25°C) for paromomycin binding (Recht *et al*., 1996). Here, a similar footprint on the A-site oligonucleotide was observed for G1494 and G1405 with gentamicin C1a (Figure 3) and C2 with an observed K_d of 2 μM (Figure 3). For gentamicin C1 a weak footprint at G1405(N7) was observed on the A-site oligonucleotide at 100 μM or 1 mM consistent with its weaker affinity for the 30S ribosomal subunit. The weakness of the protection prevents any precise determination of the K_d of gentamicin C1 for the A-site RNA at room temperature. To compare the K_ds of different gentamicins, the same experiments were performed at 4°C (Figure 3). Gentamicin C1a and C2 bind to the A-site RNA with similar affinities and K_ds of 0.01 and 0.025 μM were observed, respectively. Gentamicin C1 binds to the A-site RNA with lower affinity compared with the other two species and a K_d of 0.5 μM was observed.

The high affinity gentamicin C1a–A-site RNA complex was further studied by high resolution NMR, and its solution structure is presented below.

Structure determination of the gentamicin C1a–RNA complex

Specific binding of gentamicin C1a to the A-site RNA was characterized by monitoring the chemical shift changes of imino proton RNA resonances as a function of antibiotic concentration as previously described (Recht *et al*., 1996; Fourmy *et al*., 1998a). A 1:1 complex was formed between the A-site RNA and gentamicin C1a, consistent with the K_d of 2 μM at 25°C and the RNA concentration of 3 mM. Upon addition of gentamicin C1a, the imino protons of U1490 and G1491 are shifted downfield by 0.4 and 0.6 p.p.m., respectively.

The proton resonances of the RNA–gentamicin C1a complex were assigned using a non-labeled RNA and a ^{13}C-^{15}N-labeled RNA. Gentamicin C1a was not isotopically labeled. The free gentamicin C1a proton resonances were assigned as well.

A total of 379 Nuclear Overhauser Effect (NOE) derived distance restraints, of which 46 were intermolecular RNA–gentamicin distance restraints (Figure 4), and 111 dihedral restraints were determined (Tables I and II). Structures of

the complex were calculated using a simulated annealing protocol. A randomized array of atoms corresponding to the RNA was heated to 1000 K, and bonding, distance and dihedral restraints, and a repulsive quartic potential were gradually increased to full value over 40 ps of molecular dynamics. The molecules were then cooled to 300 K during 10 ps and subjected to a final energy minimization step that included an attractive Lennard–Jones potential. No electrostatic term was included in the target function. In the first cycle, ~90% of the final experimental restraints were used to calculate structures *de novo*. Thirty-eight of the 148 *de novo* structures converged to a low energy conformation, based on restraint violation energy. There were differences >100 kcal/mol in restraint violation energy between converged and unconverged structures. The 38 converged structures were then subjected to a second round of simulated annealing with the final set of restraints. Structural statistics for the 38 final stimulated structures are listed in Table I.

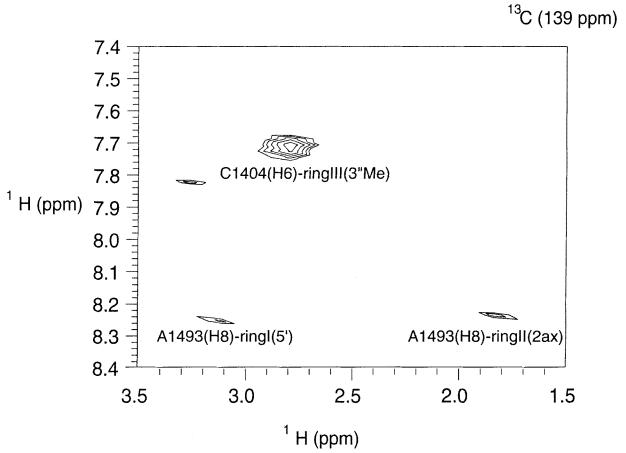

Fig. 4. 2D plane at the chemical shift of C1404 C6 (139.0 p.p.m.) from a 3D ^{13}C HMQC-NOESY experiment performed on the A-site RNA–gentamicin C1a complex at 35°C with a mixing time of 200 ms. Intermolecular NOEs between the proton H6 of C1404 with ring III of gentamicin C1a are indicated.

The overall structure of the A-site RNA is well-defined. The 38 final structures where heavy atoms of the RNA and gentamicin C1a are superimposed is shown in Figure 5A. The atomic root mean squared deviation (r.m.s.d.) of the superimposed 38 final structures is 0.76 Å (Table I).

Structure of the gentamicin C1a–RNA complex

The A-site RNA structure complexed to gentamicin C1a is formed by two A-form helical stems that close an asymmetric internal loop, which contains non-canonical pairings (Figure 5B). The upper stem is extended through a non-canonical U1406·U1495 base pair and a Watson–Crick C1407·G1494 base pair that close the internal loop. In the U1406·U1495 base pair the N3 and O4 of U1406 can form hydrogen bonds with O2 and N3 of U1495 U1406(O4)·U1495(N3), U1406(N3)·U1495(O2), U1406 (N3)·U1495(O4) and U1406(O2)·U1495(N3) are 3.7 ± 0.1, 4.8 ± 0.1, 4.3 ± 0.1 and 5.3 ± 0.1 Å apart, respectively. The hydrogen bond between the U1406(O4) and the U1495(N3) position indicates formation of a similar hydrogen bond network as the one defined in the paromomycin complex (where the N3 and O4 of U1406 hydrogen bond with O2 and N3 of U1495). A water molecule bridging the positions U1406(N3) and the U1495(O2) positions could explain the longer distance observed here (4.8 ± 0.1 Å compared with 3.5 ± 0.3 Å for the paromomycin–RNA complex) (Fourmy *et al.*, 1996).

Table I. Structural statistics and atomic r.m.s. deviations

	<SA>[a]	(SA)r	<SA> versus SA	<SA> versus (SA)r
Final forcing energies				
Distance and dihedral restraints	11.4 ± 0.3	11.1		
R.m.s.d. from experimental distance restraints (Å)[b]				
All (379)	0.0249 ± 0.0002	0.0248		
RNA (326)	0.0252 ± 0.0002	0.0250		
gentamicin C1a (7)	0.0241 ± 0.0062	0.0243		
RNA–gentamicin C1a (46)	0.0228 ± 0.0013	0.0227		
R.m.s.d. from experimental				
dihedral restraints (degrees) (111)	0.0127 ± 0.0016	0.0118		
Deviations from idealized geometry				
bonds (Å)	0.0260 ± 0.0001	0.0260		
angle (degrees)	0.0621 ± 0.0001	0.0620		
impropers (degrees)	0.0485 ± 0.0025	0.0495		
Heavy-atom r.m.s.d.				
All RNA + gentamicin C1a			0.76	0.89
Ordered RNA + gentamicin C1a[c]			0.58	0.72
gentamicin C1a			0.23	0.24
gentamicin C1a ring I			0.19	0.16
gentamicin C1a ring II			0.03	0.02
gentamicin C1a ring III			0.09	0.09

[a]<SA> refers to the final 38 simulated annealing structures, SA to the average structure obtained by taking the average coordinates of the 38 simulated annealing structures best-fitted to one another, and (SA)r to the average structure after restrained energy minimization.
[b]The 38 final structures did not contain distance violations of >0.2 Å or dihedral violations of >10°. Numbers in parentheses refer to number of restraints.
[c]RNA residues G1405 to A1410, U1490 to C1496 and all gentamicin C1a residues.

Table II. Gentamicin C1a–RNA intermolecular NOE restraints used for structure calculations

RNA		Gentamicin C1a
C1404	H6	ring III (3′′Me)
	H5	ring III (3′′Me)
	H4	ring III (3′′Me)
	H3′	ring III (3′′Me)
G1405	H8	ring III (3′′Me)
	H3′	ring III (3′′Me)
U1406	H5	ring III (3′′Me, 4′′Me, 3′′, 2′′, 5′′ax, 5′′eq)
C1407	H5	ring III (4′′Me, 5′′ax, 5′′eq)
	H4	ring III (1′′, 2′′, 4′′Me), ring II (6)
G1491	H8	ring I (2′, 3′, 4′)
	H1	ring I (6′)
	H2′	ring I (3′)
	H3′	ring I (3′, 4′)
A1492	H8	ring I (3′, 5′)
A1493	H8	ring I (5′, 6′), ring II (2ax)
	H2′	ring II (2ax, 2eq)
	H3′	ring II (3)
G1494	H1	ring III (1′′), ring II (2ax, 2eq, 6)
	H3′	ring II (2ax, 2eq)
U1495	H5	ring II (1, 2ax, 2eq, 3), ring III (1′′)
G1497	H1	ring III (3′′Me)

In the gentamicin C1a complex, A1408 and A1493 are stacked between the two stems and base paired (Figure 5B). Two families of A1408(N1)–A1493(N6) distances in the ensemble of structures are observed with the distances of 3.7 ± 0.6 Å and 4.6 ± 0.1 Å. In the former family, an A1408(N1)·A1493(N6) hydrogen bond can form. In the latter class, the A1408(N1)·A1493(N6) hydrogen bond is substituted by an A1408(N3)·A1493(N6) hydrogen bond and the average distance within these 15 structures is 3.8 ± 0.2 Å. Both hydrogen bonding schemes involve an antiparallel strand orientation of the two adenosines with anti-glycosidic torsion angles. In the free RNA, a single hydrogen bond [A1408(N1)·A1493(N6)] was identified (Fourmy *et al*., 1998b). In the paromomycin–RNA complex, A1408(N6)·A1493(N7) and A1408(N1)·A1493(N6) distances in the ensemble of structures were consistent with formation of two hydrogen bonds. The difference in the A1408·A1493 base pairing mode between the gentamicin and paromomycin complexes is difficult to interpret since fewer distance restraints in this region are available in the gentamicin–RNA complex. The A1408·A1493 pair is buckled in the ensemble of conformations, with A1493 at a 35° angle to the plane of A1408.

Formation of the A1408·A1493 pair is consistent with the protection of A1408(N1) from methylation upon binding of the gentamicin C components to the ribosome (Figure 3). The reactivities of the N1 positions of A1492 and A1493 are unaffected by antibiotic binding, and these groups are solvent-accessible on the minor groove side in the antibiotic–RNA complex. The RNA backbone is distorted by the presence of the bulged nucleotide A1492 and the non-canonical A1408·A1493 pair. This distortion results in widening of the major groove (the distance between the C1404 phosphate and A1492 phosphate is 17.17 Å in the minimized average structure as opposed to the normal A form helix distance 10.5 Å) and leads to formation of a distinct binding pocket for gentamicin (Figure 6).

Gentamicin C1a binds in the major groove of the A-site RNA within the internal loop (Figures 5A and 6). Gentamicin C1a is well defined in the ensemble of the 38 structures of the gentamicin–RNA complex (Figure 5C and Table I). When bound to the RNA, the three rings of gentamicin C1a fit into the major groove widened by the bulged A1492. Ring I (purposamine) is positioned near the A1408·A1493 pair and stacks above the base moiety of G1491 (Figures 6 and 7A). The orientation of the conserved 6′ hydrogen-bond donor, -NH_2 in gentamicin C1a, is not well defined in the solution structure. The distance between the ring I C6′ and the pro-R oxygen of the A1493 phosphate (4.6 ± 0.2 Å) is consistent with a direct contact between the 6′-amino group of ring I and the phosphate group of A1493. The 6′ nitrogen is positioned within hydrogen bonding distance to A1493(N7) (3.2 ± 0.1 Å) and G1491(N3) (3.8 ± 0.3 Å). The amino group at the 2′ position of ring I could make contacts with the phosphate atom of A1493.

Ring II (2-deoxystreptamine) spans the U1406·U1495 and C1407·G1494 base pairs. The amino groups at positions 1 and 3 of ring II make hydrogen bonds to U1495(O4) and G1494(N7), respectively (Figure 7A). The amino group at position 3 may also make contact with the phosphate between A1493 and G1494. These ring II contacts were also observed in the paromomycin–RNA complex.

Ring III (garosamine) is positioned towards the upper stem (Figures 4 and 7B). Chemical groups of ring III of gentamicin that are common among the kanamycin group antibiotics make specific contacts with universally conserved nucleotides of the A site of 16S rRNA (Figure 7B). The 2′′ hydroxyl group is within hydrogen bonding distance of G1405(O2) and U1406(O4). The nitrogen atom of the aminomethyl group at position 3′′′ of ring III forms a hydrogen bond with the G1405(N7) and may also contact the phosphate of G1405. The methyl group packs against the aromatic ring of C1404 and one face of the ribose of G1405. The 4′′′ hydroxyl forms a hydrogen bond with the phosphate between G1405 and U1406.

Several intramolecular hydrogen bonds between the different rings of gentamicin C1a were identified (Figures 5C, 7A and 7B). The amino group at the 2′ position of ring I forms a hydrogen bond with the oxygen of the hydroxyl group at the position 5 of ring II. This hydroxyl group is also hydrogen bonded to the ring III oxygen. This internal network of hydrogen bonds could help to orient the three rings for binding of gentamicin to the RNA.

Comparison of the gentamicin C1a–RNA and paromomycin–RNA complexes

Superposition of the RNA–paromomycin and RNA–gentamicin C1a complexes demonstrates the similarities and differences of the two complexes. The core RNA (residues G1405·A1410; U1490·C1496) of the two structures were superimposed and the r.m.s.d. value found is 1.48 Å. Within the superimposed structures the r.m.s.d. for rings I and II of gentamicin C1a and paromomycin are 1.28 and 0.41 Å, respectively. The superposition of the two structures (Figure 8) clearly shows that ring III of gentamicin C1a interacts with the upper stem of the A-site RNA (spanning the U1406·U1495 and G1405·C1496 base pairs) as opposed to rings III and IV of paromomycin, which interact with the lower stem (Fourmy *et al*., 1996). Rings I and II in the two

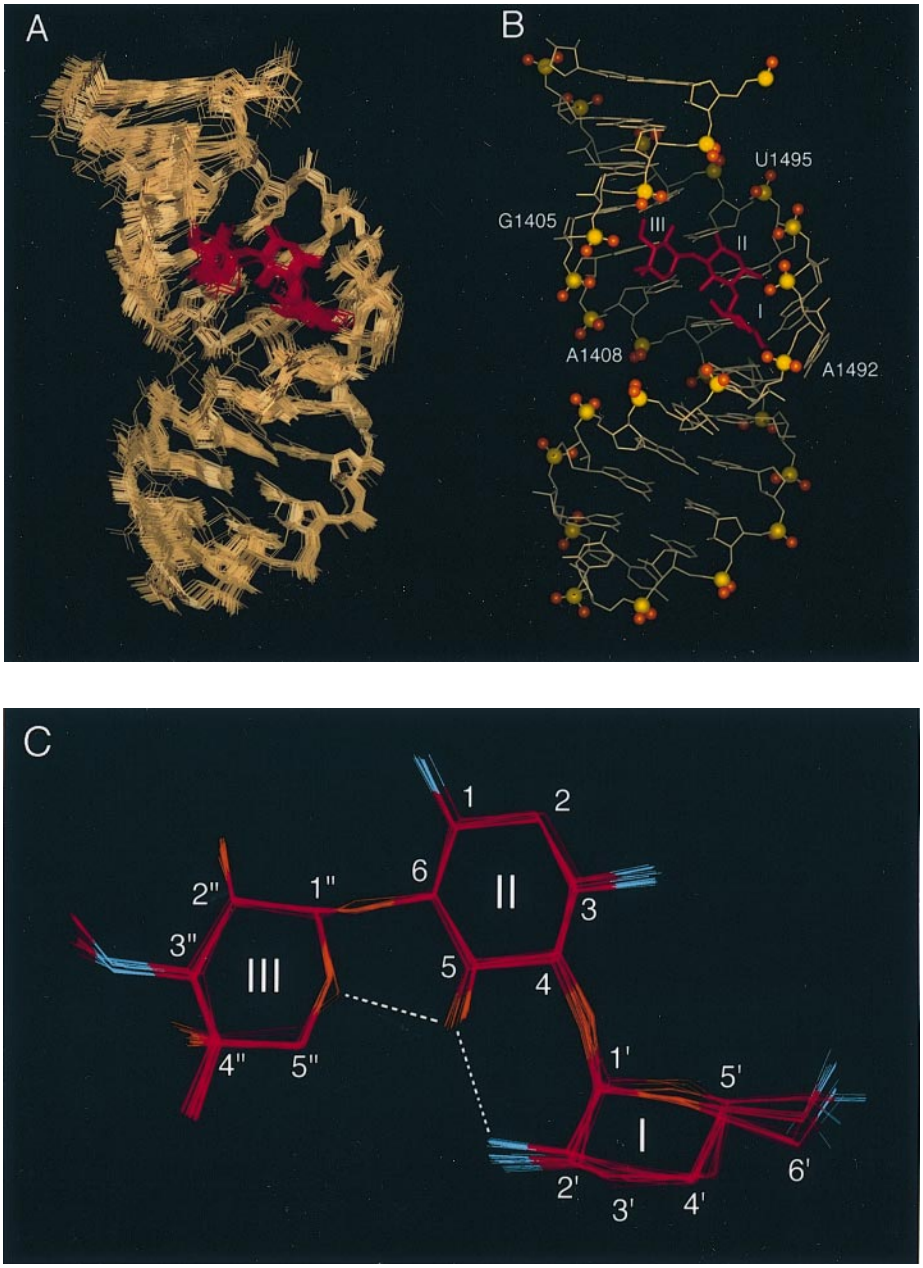

FIG. 5. (**A**) Best-fit superposition of 38 final simulated annealing structures of the A-site RNA–gentamicin C1a complex, viewed from the major groove side of the RNA. The heavy atoms have been superimposed. The RNA is shown in beige and gentamicin C1a is red. The three rings of gentamicin C1a are numbered as in Figure 1. (**B**) Single representative structure of A-site RNA–gentamicin C1a complex. All heavy atoms are displayed. The same colors as in (A) are used except that RNA phosphate groups are highlighted. (**C**) Best-fit superposition of gentamicin C1a of the 38 final structures of the A-site RNA–gentamicin C1a complex. Gentamicin C1a is in red and nitrogen atoms are highlighted in blue. Inter-ring hydrogen bonds are represented by dashed lines. Gentamicin C1a rings are labeled as in Figure 1.

complexes are similarly oriented, while the different ring II–ring III linkages lead to different ring III positions. Ring III is linked to position 6 of ring II in gentamicin C1a and to position 5 in paromomycin (Figure 1). The chemical structures of ring I in gentamicin and paromomycin differ. Nevertheless, similar specific contacts are established between ring I of the aminoglycoside and the RNA through common hydrogen-bond donor groups (Figure 7A).

The importance of the ring III–G1405 contacts in the binding of gentamicin C1a to the RNA was further investigated by mutagenesis. No binding of gentamicin C1a was observed by footprinting to a mutant RNA oligonucleotide in which the G1405·C1496 base pair was flipped to a C1405·G1496 base pair, whereas paromomycin binding was not affected by the mutation (Figure 9). These results agree with the lack of significant RNA chemical shift changes and the absence of intermolecular gentamicin–RNA NOEs upon formation of a 1:1 complex of gentamicin C1a with this mutant RNA (data not shown).

Discussion

Binding of gentamicin C components to the A site

Binding of each gentamicin C component to the A site was studied qualitatively on the 30S subunit and quantitatively on the A-site RNA oligonucleotide. Upon

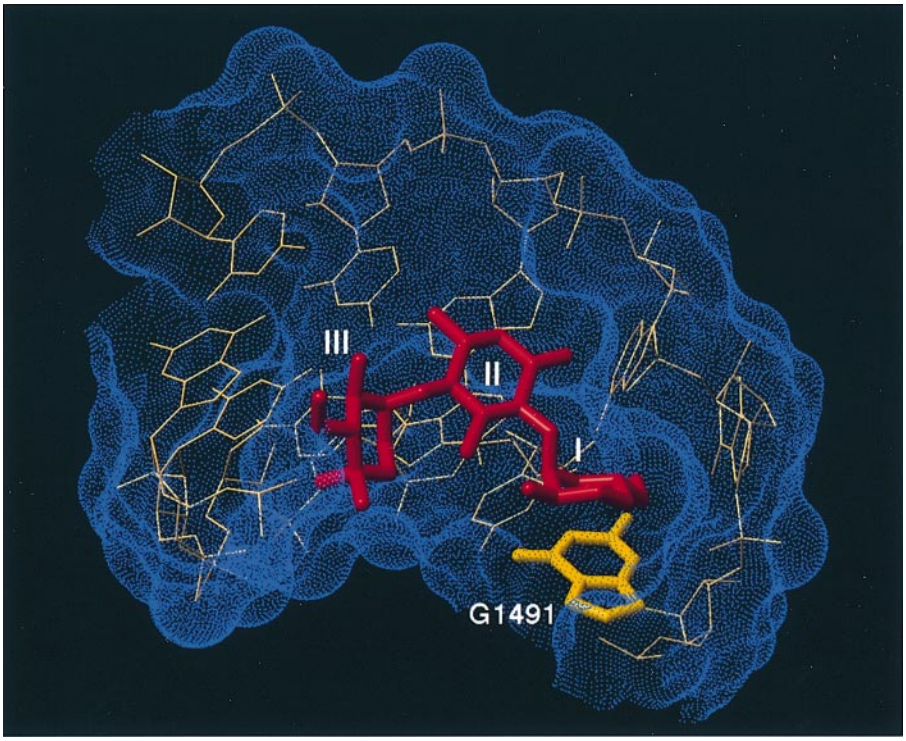

Fig. 6. Binding pocket of gentamicin in the A-site RNA. The Connolly surface of the RNA is represented by blue dots and the gentamicin C1a is red. The view is from the major groove of the RNA. The three rings of gentamicin C1a are numbered as in Figure 1. The base moiety of residue G1491 which is creating a platform for ring I binding is highlighted in yellow.

binding of each component, the same bases of the A-site RNA were protected against chemical modification by DMS, indicating a common ribosomal binding site. Quantitative analysis of the chemical footprinting of the A-site RNA showed that gentamicin C1a and C2 bind to the A site with similar affinities, C1a slightly higher than C2. Gentamicin C1 binds to A-site RNA with a 20- to 50-fold weaker affinity. Addition of a methyl group to the 6′-carbon of gentamicin C1a does not affect the affinity of the drug, whereas further introduction of a methyl group to the 6′-amino group reduces the affinity.

To understand the difference in the gentamicin–ribosome affinities, gentamicin C2 and C1 complexes with the A site were modeled based on the gentamicin C1a–A-site RNA complex structure. Gentamicin C2 has a methyl group attached to the 6′ carbon of gentamicin C1a. Since gentamicin binds deep within the major groove, rotation around the 5′ carbon and the 6′ carbon may be restricted by steric clash between the methyl group and RNA; however, this entropic penalty may be compensated by hydrophobic interactions between the methyl group and base moiety of G1491. For gentamicin C1, in which the 6′ amino group of gentamicin C2 is methylated, rotation around the 6′ carbon and 6′ nitrogen will be restricted in the binding pocket. The fixed rotation may disrupt some of the possible hydrogen bond and electrostatic interactions between the amino group and the RNA, which would result in a reduced affinity of gentamicin C1 for the RNA compared with gentamicin C1a and C2.

Structural rationale for aminoglycoside binding to the A site of 16S rRNA

The structures of the gentamicin–RNA (this work) and the paromomycin–RNA (Fourmy *et al*., 1996) complexes provide a structural framework to understand specific binding of aminoglycosides to the ribosome. Rings I and II, which contain chemical groups common among aminoglycosides that bind to the ribosomal A site, interact in the same RNA pocket (Figures 7A and 8) through a similar specific hydrogen bonding network. In both structures, amino groups 1 and 3 of ring II (2-deoxystreptamine) contact residues G1494 and U1495 with the same hydrogen bonding scheme. Rings I of gentamicin C1a and paromomycin differ at the 3′, 4′ and 6′ positions, but are similarly positioned within the same RNA-binding pocket (Figure 8). In both complexes, all polar groups of ring I are in the equatorial position allowing one face of ring I to stack upon the base moiety of G1491 (Figure 6). This type of stacking interaction was also observed in the structure of lectin–sugar complexes (Weis and Drickamer, 1996). The 2′ amino group of ring I in the gentamicin C1a–RNA complex may interact with the phosphate of residue A1493 as in the paromomycin–RNA complex (Figure 7A) (Blanchard *et al*., 1998). The 3′ and 4′ hydroxyl groups in paromomycin are substituted by hydrogens in gentamicin C1a. These hydroxyl groups make backbone contacts in the paromomycin complex that may be compensated by a hydrophobic interaction between G1491 and ring I in the gentamicin C1a complex. The hydrogen-bond donor at position 6′ (amino group for gentamicin C1a, hydroxyl group for paromomycin) contacts the phosphate of A1493 in both structures.

The comparison of the positions of rings I and II in both structures clearly reveals how similar hydrogen-bond donor groups specifically contact the RNA. This also agrees with our previous results showing that rings I and II direct the specific binding of ribostamycin and neamine to the A-site RNA (Fourmy *et al*., 1998a). We propose

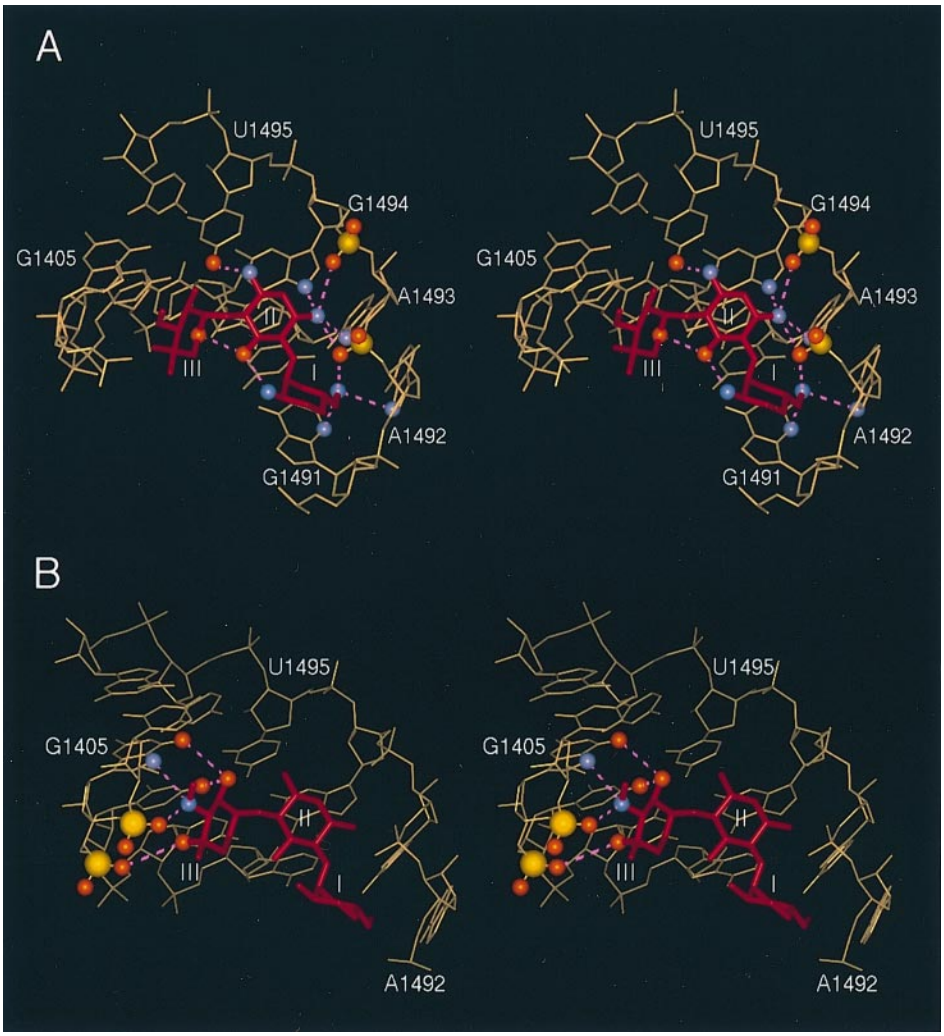

Fig. 7. RNA–gentamicin C1a contacts observed in the solution structure. (**A**) Stereo view of specific contacts made between rings I and II of gentamicin C1a and A-site RNA. The RNA is in beige, gentamicin C1a is red, and the view is looking into the major groove of the RNA. Important chemical groups are shown explicitly. The nitrogen atoms are highlighted in blue. Possible hydrogen bonding contacts are indicated by dashed lines. (**B**) Stereo view of specific contacts made between ring III of gentamicin C1a and A-site RNA. The same colors as in Figure 6A are used. Possible hydrogen bonding contacts are indicated by dashed lines.

that this is a common binding mode of all aminoglycosides that target the major groove of the A site of 16S rRNA.

Additional rings can be connected to different positions of ring II (Figure 1). Ring III of the neomycin class aminoglycosides is connected to position 5 of ring II. For the gentamicin components and kanamycins, ring III is connected to position 6 of ring II. Similar binding of rings I and II in both structures results in different binding sites for ring III of gentamicin C1a and rings III and IV of paromomycin (Figure 8). Ring III of gentamicin C1a interacts with the upper stem region (U1406·U1495 and G1405·C1496 base pairs) (Figure 7B), whereas rings III and IV of paromomycin interact with the lower stem of the A-site RNA (Fourmy *et al*., 1996). Interestingly, no antibiotics of the kanamycin class exist with four rings. The gentamicin structure shows that it would be difficult to accommodate an additional ring in a linear array in the RNA. In contrast, rings III and IV in the neomycin class are directed within the major groove of a long lower stem and are readily accommodated in the RNA complex.

Rings III and IV of paromomycin or neomycin contribute to the affinity of the drug for the rRNA (Fourmy *et al*., 1998a). In both cases, ring IV presents an additional positive charge to the RNA, increasing its affinity (Alper *et al*., 1998; Fourmy *et al*., 1998a). The contribution of gentamicin ring III to the binding affinity can be estimated to be a factor of 50 by comparing the K_ds measured for the gentamicin components with that estimated for neamine (Fourmy *et al*., 1998a). Ring III of gentamicin presents hydrogen-bond donors to the RNA (Figure 7B). The aminomethyl group in position 3″ hydrogen bonds with the N7 and phosphate of G1405. The pK_a of dimethylamine (10.7) suggests that this position should be protonated at neutral pH, but the pK_a values in the complex are not known. The 2″ hydroxyl is at hydrogen bonding distance of the O6 of G1405 and the O4 of U1406. The importance of the ring III–G1405 contacts in the binding of gentamicin components to the RNA has been confirmed by mutagenesis. A mutant RNA oligonucleotide, where the G1405·C1496 base pair was flipped to a C1405·G1496 base pair, lost affinity for gentamicin as observed by footprint experiments and NMR. Hydrogen-bond donors

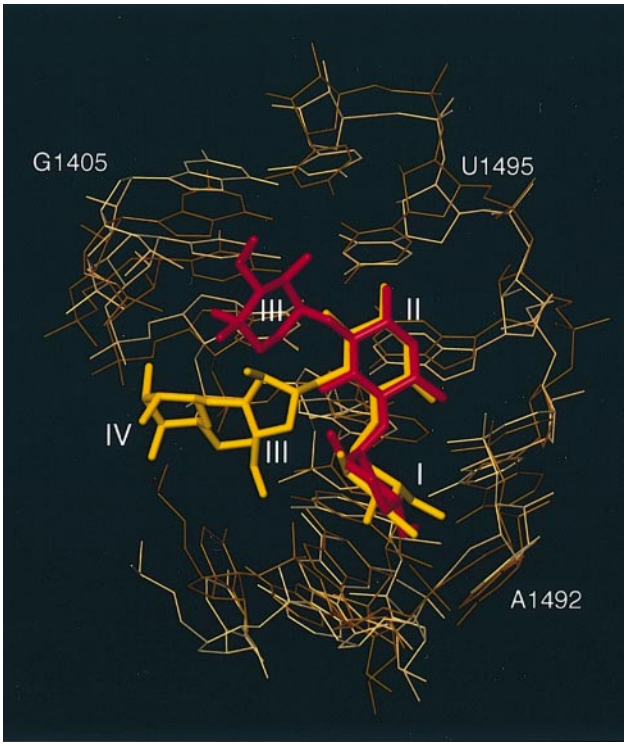

Fig. 8. Best-fit superposition of the paromomycin–RNA and gentamicin C1a–RNA complexes, viewed from the major groove side of the RNA. The heavy atoms of the core (nucleotides U1406 to A1410, and U1490 to U1495) of the RNA are superimposed. Only the core is represented. For the paromomycin–RNA complex, the RNA is represented in brown and the antibiotic in yellow. For the gentamicin C1a–RNA complex, the RNA is in tan and the gentamicin in red.

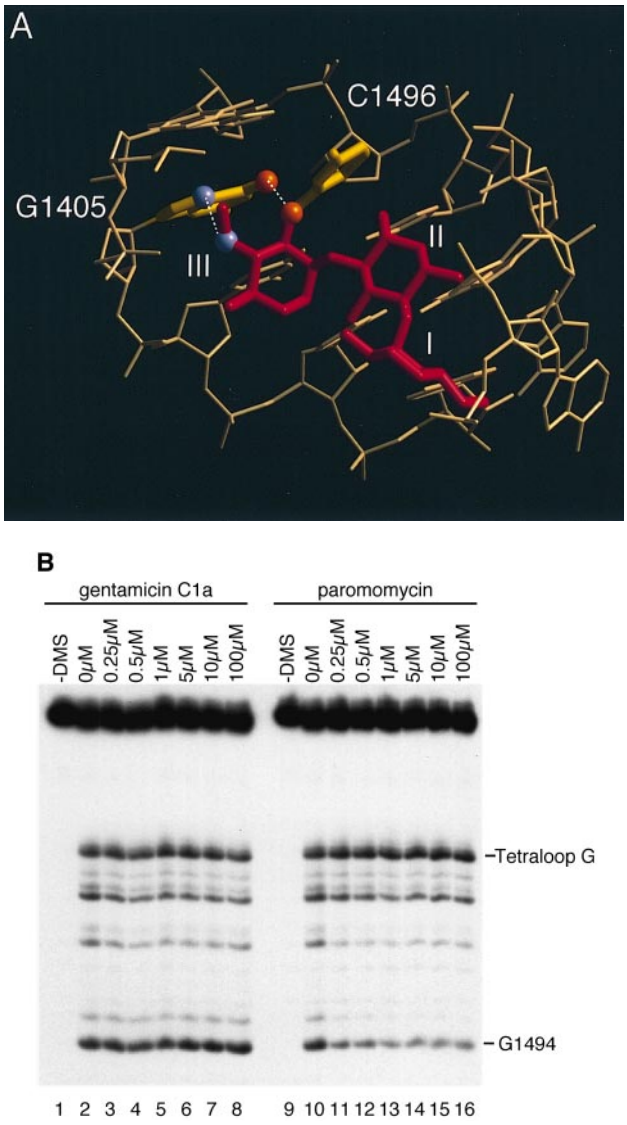

Fig. 9. (**A**) View of specific contacts made between ring III of gentamicin C1a and A-site RNA. The RNA is in tan, gentamicin C1a is red, and the view is into the major groove of the RNA. Possible hydrogen bonding contacts between G1405/C1496 base pair and ring III of gentamicin C1a are indicated by dashed lines. (**B**) Autoradiograph of DMS probing reactions on the 3′ end labeled 27 nucleotide RNA with G1405C/C1496G substitutions. In all reactions, the oligonucleotide is present at a concentration of 5 nM. Lanes 1 and 9 are control reactions with no DMS added. Lanes 3 and 10 are DMS probing reaction in the absence of antibiotics. DMS probing reactions were carried out at 25°C. Lanes 3–8 are reactions in the presence of 0.25, 0.5, 1, 5, 10 and 100 μM gentamicin C1a, respectively. Lanes 11–16 are reactions in the presence of 0.25, 0.5, 1, 5, 10 and 100 μM paromomycin, respectively.

at the 2″ and 3″ positions of ring III are common among kanamycin class aminoglycosides (Figure 1) and direct specific interaction with universally conserved nucleotides in the gentamicin C1a–RNA complex (Figure 7B).

The gentamicin–RNA structure suggests why aminoglycosides with a 4,6-substituted ring II are clinically preferred. The ring III of these aminoglycosides make additional sequence-specific contacts with the A site; in contrast, aminoglycosides with a 4,5-substituted ring II do not make additional base-specific contacts beyond rings I and II. Gentamicin–RNA contacts are apparently highly cooperative, as disruption of ring III–G1405 hydrogen bonds leads to a severe loss of affinity. The improved specificity of the gentamicin and kanamycin class aminoglycosides may better direct these drugs towards their correct ribosomal target.

Gentamicin C components and aminoglycoside resistance

Many aminoglycoside resistant bacteria confer resistance to the drug through covalent modification of the RNA or the antibiotic. Enzymatic methylation of the rRNA at A1408(N1) or G1405(N7), results in a high level resistance to specific combinations of aminoglycosides (Beauclerk and Cundliffe, 1987). Methylation of G1405(N7) confers resistance to kanamycin and gentamicin but not to paromomycin nor neomycin (Thompson *et al*., 1985; Beauclerk and Cundliffe, 1987). The structure of the gentamicin C1a–RNA complex clearly illustrates how methylation of the G1405(N7) can prevent the formation of a hydrogen bond with ring III of gentamicin in addition to creating a steric clash. No contacts between G1405 and paromomycin were observed, and mutation of the G1405·C1496 pair to C1405·G1496 did not affect paromomycin binding. The two aminoglycoside–rRNA structures readily explain the specific resistance observed for kanamycin-class aminoglycosides upon G1405 methylation.

Methylation of A1408(N1) prevents formation of the A1408·A1493 base pair which is essential for aminoglycoside binding. This modification leads to kanamycin resistance as already revealed in the paromomycin–RNA

complex and confirmed in the gentamicin C1a–RNA complex.

The enzymatic modification of aminoglycosides is the predominant resistance mechanism to this class of antibiotics (Shaw *et al*., 1993). Modification enzymes primarily target rings I and II, which direct specific interactions with the A site. Enzymatic acetylation of the conserved amino group on the ring II (position 3) of aminoglycosides was discussed previously (Fourmy *et al*., 1996). In the neomycin class antibiotics, the 6′-amino group on ring I can be acetylated. Steric hindrance prevents binding and leads to aminoglycoside resistance. Although the affinity of the 6′-acetyl gentamicin-rRNA interaction is not known, it is probably weaker than that of gentamicin C1 whose binding is affected by the steric clash of the 6′-N-methyl group with the RNA.

In the neomycin class, 3′ and 4′ hydroxyl groups of ring I are phosphorylation and adenylation targets, respectively, that would lead to steric and electrostatic penalties to complex formation. These two hydroxyls are absent in the gentamicin components and other later generation aminoglycoside antibiotics with little consequence for RNA binding. They are not targets for these classes of aminoglycoside modifying enzymes.

Aminoglycoside antibiotics and translation

Changes in the RNA conformation upon aminoglycoside binding have led to a proposal for the mechanism of action of aminoglycosides on translation. A comparison of the conformations of the A-site RNA in the free and paromomycin-bound forms showed that two universally conserved residues of the A site of 16S rRNA, A1492 and A1493, are displaced towards the minor groove of the RNA helix in the presence of the antibiotic (Fourmy *et al*., 1998b). These data and prior biophysical measurements (Karimi and Ehrenberg, 1994), suggested that the RNA conformation in the aminoglycoside complex was a high-affinity state for mRNA–tRNA recognition in the A site. The significance of this local conformational change for aminoglycoside antibiotic action can be examined by testing whether this conformational change can be triggered in the same way by the gentamicin class aminoglycosides. The high resolution structure of the gentamicin C1a–RNA complex was compared with the free form RNA and the paromomycin–RNA complex. The same displacement of A1492 and A1493 towards the minor groove was observed upon gentamicin C1a binding (Figure 8). This strongly suggests that aminoglycosides containing rings I and II act through the same mechanism despite different RNA contacts by additional rings (III and IV). Additional rings in aminoglycosides contribute to binding affinity and assist in the correct orientation of rings I and II by creating additional drug–RNA or drug–drug contacts.

The amino group at position 1 of ring II of gentamicin C1a or paromomycin is hydrogen bonded to the O4 of U1495. The binding pocket of ring III of gentamicin C1a also spans this universally conserved U1406·U1495 base pair. Mutation of U1406 to G or U1495 to G, C or A are lethal (M.I.Recht and J.D.Puglisi, unpublished results). Binding of ring II to U1495 contributes to the stabilization of a specific base-pairing pattern common to the gentamicin C1a–RNA and paromomycin–RNA complexes. This U1406·U1495 base pair geometry is different in the free RNA (Fourmy *et al*., 1998b). The role of this non-canonical base pair in ribosome function remains unknown. In this context, the mode of binding of the additional ring III of gentamicin C1a to the U1406·U1495 base pair remains of particular interest.

The structural rationale provided by this work for aminoglycoside binding to the ribosome strongly supports our proposed model for the origin of aminoglycoside antibiotic-induced miscoding. This study of the binding of different aminoglycosides to the A site of 16S rRNA provides a more precise understanding of the mode of action of this rich family of antibiotics and can help in the design of new therapeutic agents.

Materials and methods

Purification of gentamicin C components

Gentamicin C sulfate (Fluka) was converted into gentamicin base by running through Amberite IRA-400 (Fluka) column. One gram of free base gentamicin C was dissolved in 4 ml of lowerphase of isopropanol:methylenechrolide:ammonium hydroxide:water mixture (1:2:0.6:0.4) and loaded onto the silica gel (internal diameter 2 cm × 20 cm). The gentamicin components were eluted with the same solvent and the 20 ml fractions were collected. The fractions were analyzed by silicagel TLC (Whatmann; LK6 silicagel 60 Å) and detected with ninhydrin.

Chemical probing of ribosomes and oligonucleotide

Modification reactions (100 µl) with 30S subunits (10 pmol) were performed in a buffer containing 80 mM potassium cacodylate pH 7.2, 100 mM ammonium chloride, 20 mM magnesium chloride, 1 mM dithiothreitol and 0.5 mM EDTA, as previously described (Fourmy *et al*., 1998a). Primer extension of the 16S rRNA was performed as described using a DNA primer which is complementary to nucleotides 1530–1509 of 16S rRNA (Stern *et al*., 1988).

Modification reactions on the oligonucleotide used 3′ end-labeled 27 nt A-site RNA. Chemical modification reactions (300 µl) were performed in 80 mM potassium cacodylate pH 7.0, with 5 nM RNA oligonucleotide. Gentamicin components were added and modification was performed by addition of DMS (15 µl of a 1/10 dilution in ethanol) followed by incubation at room temperature for 5 min or on ice for 30 min. Reactions were stopped by ethanol precipitation. Sodium borohydride reduction and aniline-induced strand scission was performed as described (Recht *et al*., 1996). Modified RNA was resuspended in 10 µl 1 M Tris–HCl pH 8.2. Upon addition of 10 µl of freshly prepared 0.2 M $NaBH_4$, the samples were incubated on ice in the dark for 30 min. The reaction was quenched by addition of 100 µl 0.4 M NaOAc followed by ethanol precipitation. Pellets were dissolved in 20 µl 1.0 M aniline/acetate, pH 4.5 followed by incubation in the dark for 20 min at 60°C. The reaction was quenched by addition of 100 µl 0.4 M NaOAc and 100 µl phenol:chloroform:isoamyl alcohol (25:24:1) followed by vigorous mixing and centrifugation. The RNA was concentrated by ethanol precipitation of the aqueous phase and pellets were washed with 100 µl cold 70% ethanol. Cleaved fragments were separated on a 20% polyacrylamide gel, and quantitated using a PhosphorImager.

NMR sample preparation

Milligram quantities of the A-site RNA (27 nucleotides) were prepared unlabeled and uniformly ^{13}C-^{15}N-labeled by *in vitro* transcription from an oligonucleotide template and purified as described (Puglisi and Wyatt, 1995). After electro-elution and ethanol precipitation, the resuspended RNA was then dialyzed against the buffer used for the NMR experiment in a microdialysis apparatus with a 3500 MW cut-off membrane. A 1:1 complex of RNA and gentamicin C1a was prepared by monitoring the imino proton chemical shift changes. After the addition of gentamicin C1a, the NMR sample was again dialyzed against the buffer.

NMR spectroscopy

Most NMR experiments were recorded on a Varian Unity+ 500 MHz spectrometer equipped with triple resonance, *z*-gradient probes. Several NMR experiments were recorded on a Bruker DMX-750 spectrometer at the University of Wisconsin, Madison. NMR data were processed

using Varian or Felix software. NMR experiments were performed in 10 mM sodium phosphate pH 6.4. The concentrations of unlabeled RNA and uniformly ^{13}C-^{15}N-labeled RNA were 3 mM and 2.5 mM, respectively. Sample volumes were 270 µl in Shigemi NMR tubes. ^{15}N chemical shifts were indirectly referenced to the nitrogen chemical shift of $^{15}NH_4{}^+Cl^-$ in HCl (Levy and Lichter, 1979). ^{13}C chemical shifts were referenced with the known chemical shifts of the ribose carbon from the tetraloop (Varani and Tinoco, 1991).

The exchangeable and non-exchangeable protons of the unlabeled RNA were first partially assigned using standard NMR experiments. Temperature was varied (5, 10, 15, 25, 35, 45°C) to help the proton assignment. The assignment of the imino protons of the labeled RNA was complete using an HSQC experiment performed at 5°C (Kay *et al*., 1992). The hydrogen bonding patterns of the base pairs were determined from analysis of SSNOESY spectra in H_2O at different mixing times (75, 150, 300 ms) (Smallcombe, 1993). Partial assignment of the amino protons of the labeled RNA was performed with heteroTOCSY experiments (Simorre *et al*., 1995). The assignment of the nonexchangeable protons of the labeled RNA was completed using constant-time HSQC (Santoro and King, 1992), 3D-HCCH-TOCSY and 3D-HMQC-NOESY (Clore *et al*., 1990). Sequential connectivities between nucleotides in RNA were obtained by HP-COSY. The H2 protons of the adenines were assigned for the labeled RNA by correlation of the H2/H8 resonances in a 2D HCCH-TOCSY experiment (Marino *et al*., 1994).

Structure calculation

Structures were calculated using a simulated annealing protocol within the InsightII NMRArchitect package (Biosym Technologies, San Diego, CA). A randomized array of atoms corresponding to RNA was heated to 1000 K, and bonding, distance and dihedral restraints and a repulsive quartic potential were gradually increased to full value over 40 ps of molecular dynamics. The molecules were then cooled during 10 ps to 300 K and subjected to a final energy minimization step that included an attractive Lennard–Jones potential. No electrostatic term was included in the target function. Using this protocol, 25% of the structures converged, as based on restraint violation energies, and 38 of them were collected to be further refined with the final set of restraints. During refinement, molecules were heated to 1000 K and subject to 30 ps of molecular dynamics following the same protocol as above. The molecules were then cooled during 10 ps to 300 K and subject to a final energy minimization step that again included an attractive Lennard–Jones potential and no electrostatic term. A total of 379 distance restraints were used including 88 intranucleotide RNA restraints, 186 internucleotide RNA, 52 base pair hydrogen bonding restraints; no hydrogen bonding restraints were used for non-canonical base pairs. A total of 111 experimental dihedral restraints were used. Additional restraints were used to maintain chirality. The final force constants for distance restraints were 40 and 60 kcal/mol for dihedral restraints. Base pairing hydrogen bond final force constants were set to 80 kcal/mol. All color figures were generated with the program InsightII (Biosym Technologies, San Diego, CA).

RNA dihedral restraints were assigned as described (Allain and Varani, 1995). β dihedral angles were restrained from estimates of the $^3J_{P\text{-}H5'}$, $^3J_{P\text{-}H5''}$ and $^3J_{P\text{-}C4'}$ coupling constants from the HP-COSY experiment on the unlabeled RNA.

ε was also restrained from estimates of $^3J_{H3'\text{-}P}$, $^3J_{C2'\text{-}P}$ and $^3J_{C4'\text{-}P}$ from HP-COSY. Values measured in the paromomycin–RNA complex for residues outside the core where NMR data indicates no modification of the RNA structures were maintained. Constraints of 210 ± 30° (*trans*) or 260 ± 30° (*gauche*–) or 235 ± 55° (when the *trans*- or *gauche*-conformations could not be distinguished) were used.

The γ dihedral angles were constrained using estimates of $^3J_{H4'\text{-}H5'}$ and $^3J_{H4'\text{-}H5''}$ coupling constants from the ^{31}P-decoupled DQF-COSY. For a *gauche*$^+$ conformation, γ was constrained to 55 ± 30° (or ± 40°). Again, values measured in the paromomycin–RNA complex for residues outside the core where NMR data indicates no modification of the RNA structures were maintained.

The ribose sugar pucker was estimated from analysis of the H1′-H2′ coupling constants in the ^{31}P-decoupled DQF-COSY spectrum. Nucleotides with a H1′-H2′ coupling constant of >8Hz in the COSY spectrum were classified as C2′-*endo* (δ = 160 ± 30°). Nucleotides with no COSY and TOCSY crosspeaks between the H1′-H2′ protons (j <3Hz) were classified as C3′-*endo* (δ = 85 ± 30°). Some nucleotides had weak H1′-H2′ crosspeaks in the TOCSY spectrum, but not in the COSY. When a mixed population of C2′/C3′-endo conformations was observed, the ribose puckers for these nucleotides were restrained in the range of the C2′+ C3′-endo conformations during molecular dynamics.

The glycosidic torsion angle χ was determined by the intensity of the intranucleotide H8-H1′ NOE. Only one torsion angle χ (the *syn* G residue from the tetraloop) was restrained explicitly to 65 ± 30°.

Distance restraints involving non-exchangeable RNA protons were derived from visual inspection of cross-peak intensities in 50, 100, 150, 200 and 250 ms NOESY experiments. The H5/H6 cross peak of pyrimidines was used as an internal standard. NOEs were classified into three distance bound ranges: strong 1.8–2.5 Å, medium 2.5–3.5 Å and weak 3.5–5 Å (or 3.5–5.5 Å for some NOEs with exchangeable protons of the RNA, obtained from 75 and 150 ms SSNOESY experiments). In the internal loop, distances involving A1492 and A1493, the upper limit of distance range was set to 5.5 or 6Å (for NOEs involving H2 protons). The appropriate pseudoatom distance corrections were used.

Acknowledgements

The authors would like to thank Professor H.Noller and the members of his laboratory for support and discussion and in particular Chuck Merryman for providing 30S ribosomal subunits. The authors would like to also thank Michael Recht, Kam Dahlquist and Elisabetta Viani Puglisi for assistance. We also thank the Nuclear Magnetic Resonance Facility, University of Wisconsin at Madison for the use of their Bruker 750 MHz spectrometer. The coordinates of the final 38 structures have been deposited in the Brookhaven Protein Data Bank with accession number 1byj. This work was supported by grants from N.I.H. (GM51266), Packard Foundation and Lucille P.Markey Charitable Trust. S.Y. was supported by a grant from Japan Society for the Promotion of Science. D.F. was supported by a grant from Institut National de la Santé et de la Recherche Médicale.

References

Allain,F.H.-T. and Varani,G. (1995) Structure of the P1 helix from group I self-splicing introns. *J. Mol. Biol.*, **250**, 333–353.

Alper,P.B., Hendrix,M., Sears,P. and Wong,C.-H. (1998) Probing the specificity of aminoglycoside-ribosomal RNA interactions with designed synthetic analogs. *J. Am. Chem. Soc.*, **120**, 1965–1978.

Beauclerk,A.A. and Cundliffe,E. (1987) Sites of action of two ribosomal RNA methylases responsible for resistance to aminoglycosides. *J. Mol. Biol.*, **193**, 661–671.

Benveniste,R. and Davies,J. (1973) Structure–activity relationships among the aminoglycoside antibiotics: role of hydroxyl and amino groups. *Antimicrob. Agents Chemother.*, **4**, 402–409.

Blanchard,S.C., Fourmy,D., Eason,R.G. and Puglisi,J.D. (1998) rRNA chemical groups required for aminoglycoside binding. *Biochemistry*, **37**, 7716–7724.

Botto,R.E. and Coxon,B. (1983) Nitrogen-15 nuclear magnetic resonance spectroscopy of neomycin B and related aminoglycosides. *J. Am. Chem. Soc.*, **105**, 1021–1028.

Clore,G.M., Bax,A., Driscoll,P.C., Wingfield,P.T. and Gronenborn,A.M. (1990) Assignment of the side-chain 1H and 13C resonances of Interleukin-1β using double- and triple-resonance heteronuclear three-dimensional NMR spectroscopy. *Biochemistry*, **29**, 8172–8184.

Davies,J. and Davis,B.D. (1968) Misreading of ribonucleic acid code words induced by aminoglycoside antibiotics. *J. Biol. Chem.*, **243**, 3312–3316.

Davies,J., Gorini,L. and Davis,B.D. (1965) Misreading of RNA codewords induced by aminoglycoside antibiotics. *Mol. Pharmacol.*, **1**, 93–106.

Fourmy,D., Recht,M.I., Blanchard,S.C. and Puglisi,J.D. (1996) Structure of the A site of *E.coli* 16S ribosomal RNA complexed with an aminoglycoside antibiotic. *Science*, **274**, 1367–1371.

Fourmy,D., Recht,M.I. and Puglisi,J.D. (1998a) Binding of neomycin-class aminoglycoside antibiotics to the A Site of 16S rRNA. *J. Mol. Biol.*, **277**, 347–362.

Fourmy,D., Yoshizawa,S. and Puglisi,J.D. (1998b) Paromomycin binding induces a local conformational change in the A site of 16S rRNA. *J. Mol. Biol.*, **277**, 333–345.

Karimi,R. and Ehrenberg,M. (1994) Dissociation rate of cognate peptidyl-tRNA from the A-site of hyper-accurate and error-prone ribosomes. *Eur. J. Biochem.*, **226**, 355–360.

Kay,L.E., Keifer,P. and Saarinen,T. (1992) Pure absorption gradient enhanced heteronuclear single quantum correlation spectroscopy with improved sensitivity. *J. Am. Chem. Soc.*, **114**, 10663–10665.

Levy,G.C. and Lichter,R.L. (1979) Nitrogen-15 nuclear magnetic resonance spectroscopy. In *Nitrogen-15 Nuclear Magnetic Resonance Spectroscopy*. John Wiley and Sons, New York.

Marino,J.P., Prestegard,J.H. and Crothers,D.M. (1994) Correlation of adenine H2/H8 resonances in uniformly ^{13}C-labeled RNAs by 2D HCCH-TOCSY: a new tool for ^{1}H assignment. *J. Am. Chem. Soc.*, **116**, 2205–2206.

Moazed,D. and Noller,H.F. (1987a) Interaction of antibiotics with functional sites in 16S ribosomal RNA. *Nature*, **327**, 389–394.

Moazed,D. and Noller,H.F. (1987b) Chloramphenicol, erythromycin, carbomycin and vernamycin B protect overlapping sites in the peptidyl transferase region of 23S ribosmal RNA. *Biochimie*, **69**, 879–884.

Noller,H.F. (1991) Ribosomal RNA and translation. *Annu. Rev. Biochem.*, **60**, 191–227.

Puglisi,J.D. and Wyatt,J.R. (1995) Biochemical and NMR studies of RNA conformation with an emphasis on RNA pseudoknots. *Methods Enzymol.*, **261**, 323–350.

Recht,M.I., Fourmy,D., Blanchard,S.C., Dahlquist,K.D. and Puglisi,J.D. (1996) RNA sequence determinants for aminoglycoside binding to an A-site rRNA model oligonucleotide. *J. Mol. Biol.*, **262**, 421–436.

Santoro,J. and King,G.C. (1992) A constant-time 2D overbodenhausen experiment for inverse correlation of isotopically enriched species. *J. Mag. Res.*, **97**, 202–207.

Shaw,K.J., Rather,P.N., Hare,R.S. and Miller,G.H. (1993) Molecular genetics of aminoglycoside resistance genes and familial relationships of the aminoglycoside-modifying enzymes. *Microbiol. Rev.*, **57**, 138–163.

Simorre,J.P., Zimmermann,G.R., Pardi,A., Farmer,II,B.T. and Mueller,L. (1995) Triple resonance HNCCCH experiments for correlating exchangeable and non-exchangeable cytidine and uridine base protons in RNA. *J. Biomol. NMR.*, **6**, 427–432.

Smallcombe,S.H. (1993) Solvent suppression with symmetrically-shifted pulses. *J. Am. Chem. Soc.*, **115**, 4776–4785.

Stern,S., Moazed,D. and Noller,H.F. (1988) Structural analysis of RNA using chemical and enzymatic probing monitored by primer extension. *Methods Enzymol.*, **164**, 481–489.

Thompson,J., Skeggs,P.A. and Cundliffe,E. (1985) Methylation of 16S ribosomal RNA and resistance to the aminoglycoside antibiotics gentamicin and kanamycin determined by DNA from the gentamicin-producer, *Micromonospora purpurea*. *Mol. Gen. Genet.*, **201**, 168–173.

Varani,G. and Tinoco,I. (1991) Carbon assignments and heteronuclear coupling constants for an RNA oligonucleotide form natural abundance ^{13}C-^{1}H correlated experiments. *J. Am. Chem. Soc.*, **113**, 9349–9354.

Weis,W.I. and Drickamer,K. (1996) Structural basis of lectin-carbohydrate recognition. *Annu. Rev. Biochem.*, **65**, 441–473.

Woodcock,J., Moazed,D., Cannon,M., Davies,J. and Noller,H.F. (1991) Interaction of antibiotics with A- and P-site-specific bases in 16S ribosomal RNA. *EMBO J.*, **10**, 3099–3103.

Received August 7, 1998; revised and accepted September 17, 1998